Advanced probabilistic μ-analysis techniques for AOCS validation

Jean-Marc Biannic, Clément Roos, Samir Bennani, Fabrice Boquet, Valentin Preda, Bénédicte Girouart

Advanced probabilistic μ-analysis techniques for AOCS validation

J-M. Biannic[1], C. Roos[1], S. Bennani[2], F. Boquet[2], V. Preda[2] and B. Girouart[2]

***Abstract*— Monte-Carlo simulations play a key role in the current AOCS V&V process, but it is generally time-consuming and it may fail in detecting worst-case configurations, especially in the presence of rare events. In such a case, μ-analysis offers a nice alternative, although it cannot measure the probability of occurrence of the identified worst-cases, which can invalidate a control system on the basis of unlikely events. Probabilistic μ-analysis was introduced in this context 20 years ago to bridge the gap between the two techniques, but until recently no practical tools were available. This paper summarizes recent advances on this topic with a particular emphasis on practical applications to space systems. More precisely, the proposed technique is applied to evaluate AOCS controllers in the context of a challenging high accuracy satellite pointing control problem. The way the proposed tools can be integrated into the traditional AOCS V&V process and used to tighten the V&V analysis gap is also highlighted.**

I. INTRODUCTION

Novel lightweight materials and deployable structures allow to perform an increasingly wide variety of on-orbit services, which results in stronger interactions between the spacecraft flexible structures and fuel sloshing in the reservoirs. Efficient Attitude & Orbit Control Systems (AOCS) must then be designed to ensure a high pointing accuracy. This requires a robust control architecture, but also adequate verification and validation (V&V) methods to assess the mission risk and check if performance is guaranteed regardless of the uncertainties and disturbances affecting the system.

Monte-Carlo (MC) simulations [8], [10] are the preferred validation means in the space industry. They are able to quantify the probability of sufficiently frequent phenomena, but only provide only soft bounds [24] and become very time-consuming to detect rare (but critical) events. On another side, deterministic and simulation-free alternatives exist and have now reached a good level of maturity, as is the case for μ-analysis [7], [19]. But unlike MC simulations, if worst-case scenarios are no longer missed, their probability of occurrence is also not measured, which can invalidate an AOCS on the basis of very rare and therefore extremely unlikely events [2], [12], [22].

Research to fill the gap between these two approaches is still at a very early stage and only few practical tools are available, although this issue was identified 20 years ago by [9]. This is all the more surprising since the validation process currently accounts for up to 80% of the AOCS total development time, and is becoming longer as the space missions become increasingly complex. In this context, this paper builds on the work of [22], [6], [2], [23] on probabilistic μ-analysis and its ambitions are twofold. First, develop cheaper and reliable tools to improve the characterization of rare but nonetheless possible events, so as to tighten the aforementioned V&V analysis gap. Second, apply these tools to a challenging high accuracy satellite pointing control problem to show how they can be integrated into the traditional AOCS V&V cycle, so as to improve the current industrial standard and fasten the validation process.

The latest advances in probabilistic μ-analysis are first presented in Section II. The resulting computational tool is then described in Section III. It is finally applied in Sections IV and V to a challenging and realistic AOCS benchmark.

II. LATEST ADVANCES IN PROBABILISTIC μ

A. Problem statement

Let us consider a continuous-time uncertain linear time-invariant system (usually including control laws):

$$\begin{cases} \dot{x} = A(\delta)x + B(\delta)u \\ y = C(\delta)x + D(\delta)u \end{cases} \tag{1}$$

where the parametric uncertainties $\delta = (\delta_1, \ldots, \delta_N) \in \mathbb{R}^N$ are independent random variables with probability density functions $f = (f_1, \ldots, f_N)$. It is assumed that $A(\delta)$, $B(\delta)$, $C(\delta)$, $D(\delta)$ are polynomial or rational functions of the δ_i. As a result, system (1) can be transformed into a linear fractional representation (LFR) as in Fig. 1 (right): the uncertainties are separated from the nominal (closed-loop) system $M(s)$ and isolated in a block-diagonal operator $\Delta = \text{diag}(\delta_1 I_{n_1}, \ldots, \delta_N I_{n_N})$, where I_{n_i} is the $n_i \times n_i$ identity matrix. This paper focuses on real uncertainties, but complex uncertainties and neglected dynamics can also be considered.

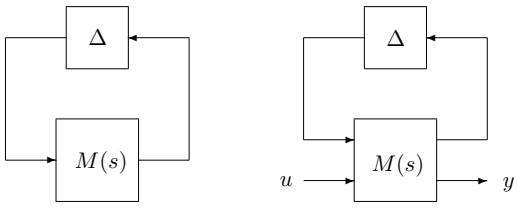

Fig. 1. Standard interconnections for robust stability (left) and worst-case performance (right) analysis

The set of matrices with the same block-diagonal structure as Δ is denoted $\mathbf{\Delta}$. It is assumed that the uncertainties are normalized, so that the subset $\mathcal{B}_{\mathbf{\Delta}}$ of $\mathbf{\Delta}$ defined as $\mathcal{B}_{\mathbf{\Delta}} = \{\Delta \in \mathbf{\Delta} : \overline{\sigma}(\Delta) < 1\} = \{\Delta \in \mathbf{\Delta} : |\delta_i| < 1, i \in [1, N]\}$ corresponds to the set of physically meaningful uncertainties. With these notations in mind, two main problems can be solved using probabilistic μ-analysis:

[1] Information Processing and Systems Department, ONERA - The French Aerospace Lab, Toulouse, France, {croos,biannic}@onera.fr

[2] ESTEC, European Space Agency, Noordwijk, The Netherlands, {samir.bennani,valentin.preda,benedicte.girouart}@esa.int

Problem 2.1 (Probabilistic robust stability): Compute the probability $\overline{P}_{\mathbf{\Delta},f}(M(s))$ that the interconnection of Fig. 1 (left) is unstable when $\Delta \in \mathcal{B}_{\mathbf{\Delta}}$.

Problem 2.2 (Probabilistic worst-case H_∞ performance): Given a performance level $\gamma > 0$, compute the probability $\overline{P}^{\gamma}_{\mathbf{\Delta},f}(M(s))$ that $\|\mathcal{T}_{u\to y}(s,\Delta)\|_\infty > \gamma$ on Fig. 1 (right) when $\Delta \in \mathcal{B}_{\mathbf{\Delta}}$, where $\mathcal{T}_{u\to y}(s,\Delta)$ is the transfer from u to y.

Once computed, these probabilities can be confronted to a given tolerance level ϵ, so as to validate or reject the considered control system, depending on whether $\overline{P}_{\mathbf{\Delta},f}(M(s))$ and $\overline{P}^{\gamma}_{\mathbf{\Delta},f}(M(s))$ are lower or higher than ϵ.

Remark 2.1: The uncertainties being bounded, their probability distributions must be supported on a bounded interval. Uniform and truncated normal distributions are often used.

B. Probabilistic robust stability

Classical μ-analysis [7] aims at computing the robust stability margin k_r, which satisfies the following properties:

- the interconnection of Fig. 1 (left) is stable for all $\Delta \in k_r\mathbf{\Delta} = \{\Delta \in \mathbf{\Delta} : |\delta_i| < k_r, i \in [1,N]\}$,
- for all $k > k_r$, there exists at least one $\Delta \in k\mathbf{\Delta}$ such that the interconnection is unstable.

This defines an uncertainty box centered at 0 and of radius k_r, which touches the instability domain and where stability is guaranteed. So if $k_r < 1$, there are parts of the uncertainty domain $\mathcal{B}_{\mathbf{\Delta}}$ that can be stable or unstable, but for which nothing can be concluded. This is illustrated in Fig. 2, which corresponds to the simple example of [6] with 2 normalized uncertainties. In this particular case, the stability and instability domains (in light/dark green and red respectively) can be calculated analytically. The domain $k_r\mathbf{\Delta}$ where stability is guaranteed by μ-analysis is the light green box, and it is clear that there are both stable and unstable zones outside this area, where no information is available at this stage.

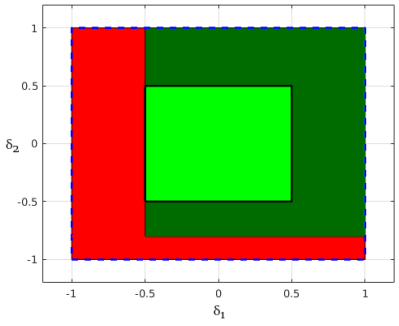

Fig. 2. Guaranteed stability domain (light green) obtained with μ-analysis

Remark 2.2: Computing k_r is in general NP-hard, so lower and upper bounds are computed instead. Much work has been done to reduce the gap between these bounds, and many efficient algorithms are now available [20]. It can thus usually be assumed that the (almost) exact value of k_r can be computed with a reasonable computational time.

A branch-and-bound (B&B) algorithm can be used to explore the whole uncertainty domain. The idea is to partition $\mathcal{B}_{\mathbf{\Delta}}$ into smaller boxes until each box has guaranteed stability or is sufficiently small to be neglected [13]. Taking the union of the boxes with guaranteed stability leads to an approximation $D_s \in \mathcal{B}_{\mathbf{\Delta}}$ of the exact stability domain. In practice, this approximation is usually quite accurate, as can be seen here by comparing the green areas in Fig. 2 and 3.

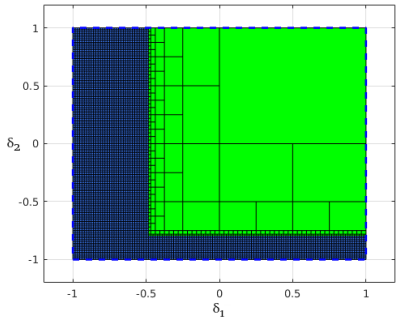

Fig. 3. Guaranteed stability domain (light green) obtained with B&B

This strategy can however result in a significant computational time for large-scale problems. In particular, the boxes where the uncertain system is unstable are never identified as such by the algorithm, since μ-analysis requires to start with a nominally stable system. They are partitioned until they reach a negligible size, which leads to unnecessary box generations. This is materialized in Fig. 3 by the use of the blue color to represent these very small undetermined boxes. But this issue can be addressed easily. μ-analysis indeed detects when the poles of the nominally stable system $M(s)$ reach the imaginary axis as the size of Δ increases. The same strategy can be applied to a nominally unstable system. Integrated into the previous B&B scheme, this directly yields a domain $D_{\bar{s}}$ of guaranteed instability.

The domain D_s of guaranteed stability conveniently takes the form of a finite union of disjoint boxes $D_s^{(k)}$:

$$D_s = \bigcup_k D_s^{(k)} \text{ where } D_s^{(k)} = [\underline{\delta}_1^{(k)}, \overline{\delta}_1^{(k)}] \times \cdots \times [\underline{\delta}_N^{(k)}, \overline{\delta}_N^{(k)}]$$

making the associated probability $p(D_s)$ easy to compute:

$$p(D_s) = \sum_k \Pr(\underline{\delta}_i^{(k)} \le \delta_i \le \overline{\delta}_i^{(k)}, i = 1,\dots,N) \quad (2)$$

$$= \sum_k \prod_{i=1}^{N} \int_{\underline{\delta}_i^{(k)}}^{\overline{\delta}_i^{(k)}} f_i(\delta_i) d\delta_i \quad (3)$$

The same applies to $D_{\bar{s}}$, which finally leads to both lower and upper bounds on the exact probability $\overline{P}_{\mathbf{\Delta},f}(M(s))$ of instability, thus solving Problem 2.1:

$$p(D_{\bar{s}}) \le \overline{P}_{\mathbf{\Delta},f}(M(s)) \le 1 - p(D_s) \quad (4)$$

The considered control system can then be either validated if $1 - p(D_s) < \epsilon$ or rejected if $p(D_{\bar{s}}) > \epsilon$, where ϵ is the tolerance level introduced in Section II-A. In practice, B&B is executed until the gap between the bounds becomes small enough and one of the two previous conditions occurs. The uncertainty domain is finally partitioned as follows:

$$\mathcal{B}_{\mathbf{\Delta}} = D_s \cup D_{\bar{s}} \cup D_{s_u} \quad (5)$$

where D_{s_u} denotes the domain of undetermined stability, with probability $p(D_{s_u})$. The B&B algorithm can indeed

only approximate D_s and $D_{\bar{s}}$, and not compute them exactly. The application to the academic example of [6] is shown in Fig. 4, and it can be seen that very good approximations of the exact stability and instability domains are obtained.

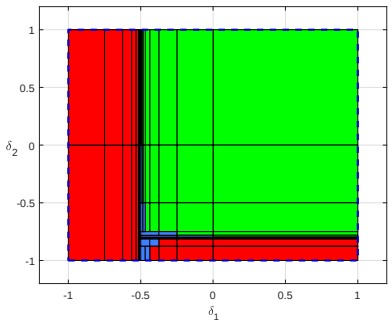

Fig. 4. Domains of guaranteed stability D_s (green), guaranteed instability $D_{\bar{s}}$ (red) and undetermined stability D_{s_u} (blue) obtained with B&B

Remark 2.3: When applying B&B, the boxes can be divided along the direction with the highest μ-sensitivity (*i.e.* corresponding to the uncertainty with the greatest influence on stability, see [5]), instead of the longest edge as usually done. This significantly reduces the number of boxes and the computational time in most cases [22], [11]. This is observed here by comparing the number of green boxes in Fig. 3 and 4, obtained without and with the μ-sensitivities respectively.

C. Probabilistic worst-case H_∞ performance

As with robust stability, B&B is combined with μ-analysis to compute domains of guaranteed performance satisfaction D_γ and guaranteed performance violation $D_{\bar{\gamma}}$, as well as the associated probability measures $p(D_\gamma)$ and $p(D_{\bar{\gamma}})$. This leads to bounds on the exact probability $\overline{P}^{\gamma}_{\mathbf{\Delta},f}(M(s))$ of non-performance, thus solving Problem 2.2:

$$p(D_{\bar{\gamma}}) \leq \overline{P}^{\gamma}_{\mathbf{\Delta},f}(M(s)) \leq 1 - p(D_\gamma) \tag{6}$$

Performance is guaranteed on a given box D, *i.e.* $D \in D_\gamma$, if:

$$\max_{\Delta \in D} \|\mathcal{T}_{u\to y}(s,\Delta)\|_\infty \leq \gamma \tag{7}$$

This can be reformulated as a skew-μ problem using the main loop theorem [15] and solved using existing μ-based tools [19]. On the other hand, checking if non-performance is guaranteed on D, *i.e.* if $D \in D_{\bar{\gamma}}$, requires to solve:

$$\min_{\Delta \in D} \|\mathcal{T}_{u\to y}(s,\Delta)\|_\infty > \gamma \tag{8}$$

This is a minimax problem, which cannot be directly reformulated as a skew-μ problem as above. To address this issue, a sufficient condition for inequality (8) to hold is introduced in [22], in the form of a skew-μ calculation involving the inverse transfer $\mathcal{T}^{-1}_{u\to y}(s,\Delta)$. It is very efficient from a computational point of view, but it may introduce conservatism, although this is usually not the case in practice. The main limitation is that this condition is restricted to a scalar performance channel, i.e. $u \in \mathbb{R}$ and $y \in \mathbb{R}$ in (1). It can then be integrated into a B&B scheme as for stability, which leads to a partition of the uncertainty domain $\mathcal{B}_{\mathbf{\Delta}}$:

$$\mathcal{B}_{\mathbf{\Delta}} = D_\gamma \cup D_{\bar{\gamma}} \cup D_{\gamma_u} \tag{9}$$

where D_{γ_u} is the domain of undetermined performance.

III. A NEW COMPUTATIONAL TOOL

All the results and algorithms presented in Section II have been implemented in the Matlab function `mupb` available at `w3.onera.fr/smac/smart_download`. The latter solves Problems 2.1 and 2.2 by computing *guaranteed* lower and upper bounds on the probabilities $\overline{P}_{\mathbf{\Delta},f}(M(s))$ and $\overline{P}^{\gamma}_{\mathbf{\Delta},f}(M(s))$ with the desired accuracy. It is fully compatible with the Generalized State-Space (GSS) Library of the SMAC Toolbox [3], which offers a powerful and user-friendly way to model LFR, including the ability to define probability distributions for parametric uncertainties. This library is itself compatible with the standard `uss` object of the Robust Control Toolbox, and it provides automated tools to convert `uss` objects to `gss` objects, as well as to incorporate probability distributions initially not present in `uss` objects. Finally, the function `mupb` is also fully interfaced with the Skew Mu Analysis Robustness Tools (SMART) Library of the SMAC Toolbox [19], which allows the user to benefit from a number of state-of-the-art μ-analysis based algorithms. It can be called quite easily as follows:

```
[pbnds,domout]=mupb(gsys,pb,domin,options);
```

where:

- `gsys` is a `gss` object describing the LFR of Fig. 1,
- `pb` specifies if Problem 2.1 or 2.2 is to be solved,
- `domin` can be used to provide an initial description of D_s, $D_{\bar{s}}$, D_{s_u}, D_γ, $D_{\bar{\gamma}}$ and D_{γ_u} coming from a previous call to `mupb`,
- `options` contains tuning parameters related to the stopping criterion of the B&B algorithm, the use of μ-sensitivities and the accuracy of the μ computation,
- `pbnds` gives the guaranteed bounds on $\overline{P}_{\mathbf{\Delta},f}(M(s))$ and $\overline{P}^{\gamma}_{\mathbf{\Delta},f}(M(s))$,
- `domout` provides the final list of boxes which make up D_s, $D_{\bar{s}}$, D_{s_u}, D_γ, $D_{\bar{\gamma}}$ and D_{γ_u} (same format as `domin`).

IV. BENCHMARK DESCRIPTION

As already emphasized in the introduction, pointing performances are continuously more demanding on both scientific and observation space missions of future generations [21]. In the presence of uncertainties, performances degradation remains very challenging to quantify reliably as it results from complex interactions between external perturbations and structural flexible modes of the spacecraft at very specific frequencies. Inspired by previous works presented in [21], [18], [4], the proposed benchmark focuses on the effects on pointing accuracy of micro-perturbations induced by a Solar Array Drive Mechanism (SADM) on a spacecraft. Since coupling effects remain limited, a single axis case of a spacecraft attitude control system is considered next.

A. Model description

The system under consideration illustrated by Fig. 5 is essentially composed of a main body, two solar arrays, an isolated payload and a wheel whose mass and inertia are neglected here. Let us denote $X = [\theta \;\; x_{SA_1} \;\; x_{SA_2} \;\; x_P]'$ the

position vector of the plant where θ is the pointing error. Using the M-D-K formalism the model is then described as:

$$\begin{bmatrix} \dot{X} \\ \ddot{X} \end{bmatrix} = \begin{bmatrix} 0 & I \\ -M^{-1}K & -M^{-1}D \end{bmatrix} \begin{bmatrix} X \\ \dot{X} \end{bmatrix} + M^{-1}W \begin{bmatrix} \Gamma_B \\ \Gamma_{SA} \end{bmatrix} \quad (10)$$

where the generalized inertia, damping and stiffness matrices are respectively defined as:

$$M = \text{diag}(J_B, J_{SA_1}, J_{SA_2}, J_P) = 10^2 \times \text{diag}(13, 21, 22, 5)$$

$$\begin{matrix} D = S(V_D) \\ K = S(V_K) \end{matrix} \quad \text{with: } S(V) = \begin{bmatrix} \text{sum}(V) & -V' \\ -V & \text{diag}(V) \end{bmatrix}$$

$$\text{and: } \begin{matrix} V_D = [D_{SA_1} \ D_{SA_2} \ D_P]' = 10^2 \times [0.5 \quad 0.5 \quad 8]' \\ V_K = [K_{SA_1} \ K_{SA_2} \ K_P]' = 10^5 \times [1 \quad 1 \quad 200]' \end{matrix}$$

Finally, the input matrix $W = \begin{bmatrix} 1 & 0 & 0 & 0 \\ 0 & 1 & 1 & 0 \end{bmatrix}'$ distributes the control torque Γ_B applied to the main body and the input perturbation torques $\Gamma_{SA} = \Gamma_{SA_1} = \Gamma_{SA_2}$ which, for simplicity, are assumed to affect similarly the 2 solar panels.

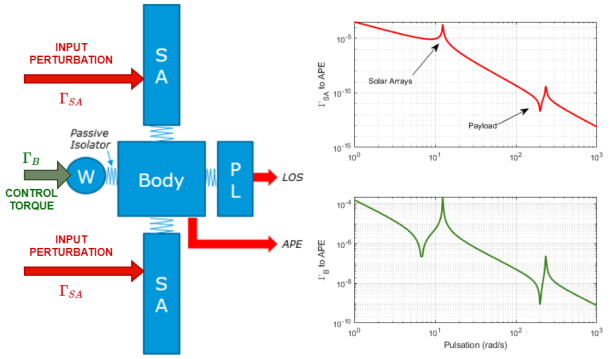

Fig. 5. Simplified view of the nominal plant

Uncertainties mainly affect the first 3 elements of M:

$$\begin{cases} J_B &= (1 + 0.1\,\delta_0) J_{B_0} \\ J_{SA_1} &= (1 + 0.2\,\delta_1) J_{SA_{1_0}} \\ J_{SA_2} &= (1 + 0.2\,\delta_2) J_{SA_{2_0}} \end{cases} \quad (11)$$

where the δ_i denote normalized uncertain parameters. Thus, the characteristics of the first two flexible modes vary significantly (see Table I), which requires a robust control design.

Element	Damping	Pulsation (rad/s)
SA1	$[1.6\,,\ 1.8] \times 10^{-3}$	$[6.35\,,\ 7.39]$
SA2	$[3.0\,,\ 3.3] \times 10^{-3}$	$[11.9\,,\ 13.1]$
Payload	$[4.7\,,\ 4.8] \times 10^{-3}$	$[231\,,\ 238]$

TABLE I
FLEXIBLE MODES CHARACTERISTICS

The particular structure of equation (10) where the uncertainties, through M^{-1}, clearly enter the model in a rational way, strongly suggests the use of the LFT framework. Either using `uss` or `gss` objects [3], a minimal LFR $\mathcal{F}_u(G(s), \Delta)$, with $\Delta = \text{diag}(\delta_0, \delta_1, \delta_2)$ is readily obtained and can be integrated in a robust $\mathcal{H}_\infty$ control design scheme (Fig. 6). In this scheme $A(s) = (1+0.05s)^{-1}$ denotes the actuator model while the W_{XX} are the standard input/output weighting functions of the $\mathcal{H}_\infty$ framework. Here, the most specific ones are $W_{SA}(s)$ and $W_{APE}(s)$ which respectively shape the disturbance inputs interacting with the flexible modes of the solar panels and the absolute pointing error (APE) output. Based on previous work introducing relevant metrics for pointing accuracy [16], [14], [17], it appears that such a requirement can be quantified via the $\mathcal{H}_\infty$ norm of a weighted transfer. In this application, the proposed weighting functions, extracted from [4]:

$$W_{SA}(s) = \left(\frac{1.245 \times 10^{-2}\, s}{s^2 + 1.245 \times 10^{-2}\, s + 155} \right)^2$$

$$W_{APE}(s) = 2 \times 10^5 \times \frac{300s + 1}{3s + 1}$$

are such that the main performance requirement is met when:

$$\gamma_{ape} = \|\mathcal{T}_{w_{SA} \to z_{APE}}(s)\|_\infty \leq 1 \quad (12)$$

$W_{SA}(s)$ is a selective bandpass filter that excites the system near $12.5\,rad/s$, while $W_{APE}(s)$ is a highpass filter.

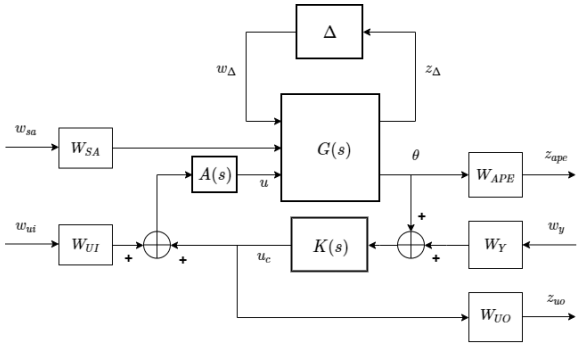

Fig. 6. Weighted LFT-based closed-loop model

B. Controller design

Control design is performed in two steps. A preliminary PD-like first order controller is initially designed by a modal-based approach that robustly stabilizes the double integrator of the plant for all admissible δ_i. Next, the poor performance level of this initial controller is improved by a multi-model structured $\mathcal{H}_\infty$ design approach based on `systune` as proposed in [1] for example. Since the optimization problem is strongly nonconvex, the routine is initialized by the robustly stabilizing PD controller using a non-minimal third order augmentation. With this approach, a very low-order controller is rapidly obtained despite the relatively high order of the weighted design interconnection ($n = 17$). As is visible on the Bode plot of Fig. 7, this controller exhibits poorly damped poles and zeros near $12.5\,rad/s$ and $13\,rad/s$ respectively. These are the necessary ingredients to ensure a good rejection of the input perturbations on the solar panels. However, with such a low-order solution, it was not possible to ensure *a priori* that the performance requirement (12) is met for all admissible uncertainties.

C. Preliminary robustness analysis

A preliminary analysis is realized to evaluate the robustness of the pointing performance. This is first achieved by a standard evaluation of the $\mathcal{H}_\infty$ norm for 2000 randomly generated configurations according to a uniform distribution

for each parameter. The results are presented in Fig. 8 which also displays a worst-case plot detected by skew μ analysis. At this stage, the controller seems to be validated by the standard MC approach, while it is invalidated by μ-analysis.

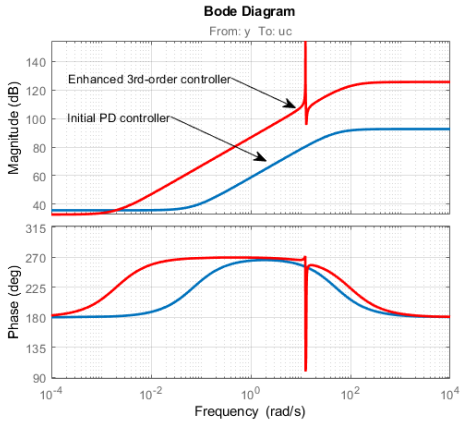

Fig. 7. Controllers Bode diagrams

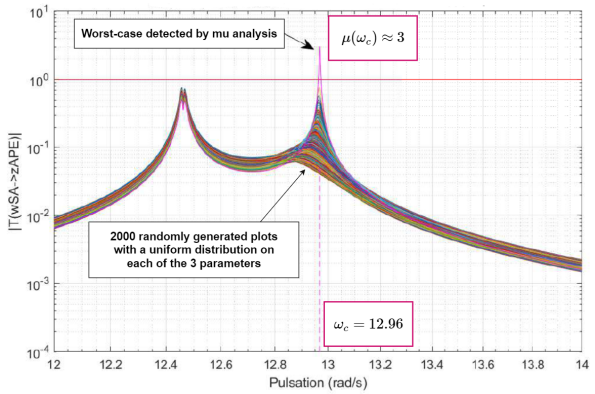

Fig. 8. Robust performance: Monte-Carlo vs skew μ analysis

Method	**# samples**	$\mathcal{P}(\gamma_{\mathbf{ape}} > \mathbf{1})$	$\gamma^{\star}_{\mathbf{ape}}$	**CPU time**
MC	5000	0	0.76	20 s
MC	25000	2.4×10^{-4}	1.34	100 s
MC	50000	1×10^{-4}	1.76	190 s
MC	100000	9×10^{-5}	1.89	410 s
MC	200000	9.5×10^{-5}	2.23	860 s
skew μ	NA	NA	3.08	6 s

TABLE II

REFINED MONTE-CARLO ROBUSTNESS ANALYSIS

A refined and time consuming[1] MC analysis (see Table II) is required to obtain a tight approximation of the probability of failure $\mathcal{P}(\gamma_{\mathbf{ape}} > \mathbf{1}) \approx \mathbf{10^{-4}}$, which, as proven by skew μ analysis, is not zero.

V. APPLICATION OF STOCHASTIC μ-ANALYSIS

In this example, involving a low probability of failure (however invalidated by μ-analysis), MC techniques are not well suited. The new computational tool presented in Section III is then used here to address Problem 2.2.

[1]All computations have been performed on a standard laptop equipped with a processor Intel i5-8400H, 2.50GHz with 16Gb RAM installed.

A. Initial characterization of the performance regions

Considering first uniform distributions for all parametric uncertainties, the routine `mupb` is called on the uncertain (but robustly stable) closed-loop LFT model to evaluate the performance regions D_{γ}, $D_{\bar{\gamma}}$ and D_{γ_u} from which guaranteed probability bounds are deduced. A stopping criterion (see Section III) is fixed such that a good compromise is obtained between accuracy and computational time as illustrated in Table III. Note that in both cases, the computed intervals confirm the previous Monte-Carlo analysis.

CPU time	55 s	270 s
$\mathcal{P}(\gamma_{\mathbf{ape}} > \mathbf{1})$	$[0.53\,10^{-4}\ \ 2.02\,10^{-4}]$	$[[0.86\,10^{-4}\ \ 1.4\,10^{-4}]$

TABLE III

GUARANTEED PROBABILITY BOUNDS OBTAINED WITH MUPB

A cross-sectional visualization (with $\delta_0 = 1$) of the performance regions in the plane $< \delta_1 \times \delta_2 >$ is presented in Fig. 9, for the highest accuracy case. The undetermined region (visualized in blue) is reasonably small.

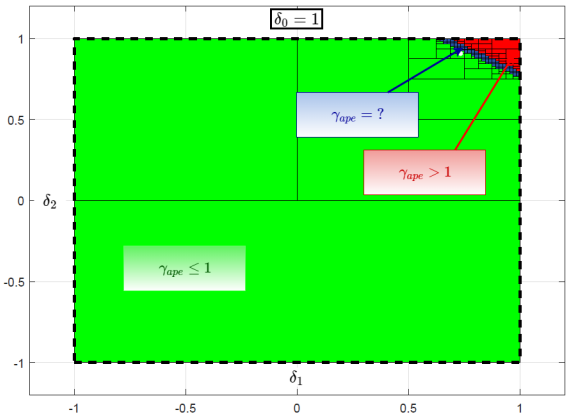

Fig. 9. Cross-sectional visualization ($\delta_0 = 1$) of the performance regions

B. Probability levels cheap reassessment

Beyond the guaranteed results (through hard bounds on the probability of failure) provided by probabilistic μ-analysis, the most interesting feature is that it also provides a set of regions (see Fig. 9) which can be re-used at a very low cost to evaluate new probability levels for any distribution of the uncertain parameters in their respective intervals. In this application this is achieved by considering truncated normal distributions with the same varying standard deviation $\sigma \in [0.3\,,\ 5]$ for each parameter. The results, obtained in a few seconds, are presented in Fig. 10 which shows the evolution of the guaranteed upper and lower bounds as a function of σ.

As expected a convergence towards the bounds obtained with uniform distribution (black solid and dashed lines) is observed when $\sigma \to \infty$. Conversely, for small values of σ, the probability levels become unsurprisingly so small that they could not be detected by any MC type approach. In this respect, the proposed approach clearly bridges a gap between classical methods and μ-analysis. It also permits to highlight a relationship between the probability to be demonstrated and the characteristics of the uncertainties. For example, if

the targeted probability of failure is 10^{-6}, then the controller is validated when $\sigma \leq 0.45$.

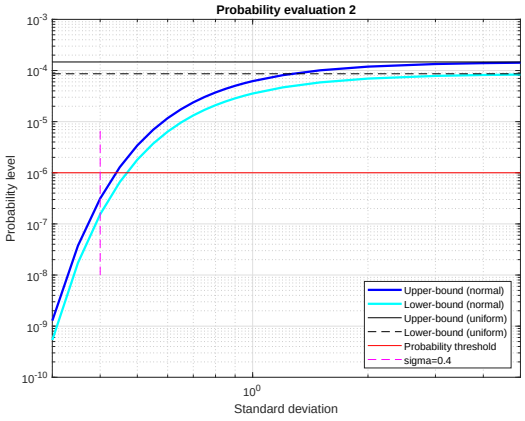

Fig. 10. Probability evaluation *w.r.t* standard deviation

VI. CONCLUSIONS AND PERSPECTIVES

Based on recent algorithmic advances on probabilistic μ-analysis and a new Matlab-based implementation, promising results have been obtained on a realistic benchmark, thus opening the way towards more efficient design-and-validation cycles as suggested in Fig. 11. As emphasized in Subsection V-B, a very interesting feature of the proposed approach is to enable very fast iterations between the probability level and the uncertainties characterization. At a medium cost, uncertainty resizing is also possible. Future work will also be devoted to more advanced evaluations involving several criteria simultaneously such as $\mathcal{H}_\infty$ performance on multiple channels but also robust gain and phase margins. Next, extensions to uncertain time-varying parameters should also be considered.

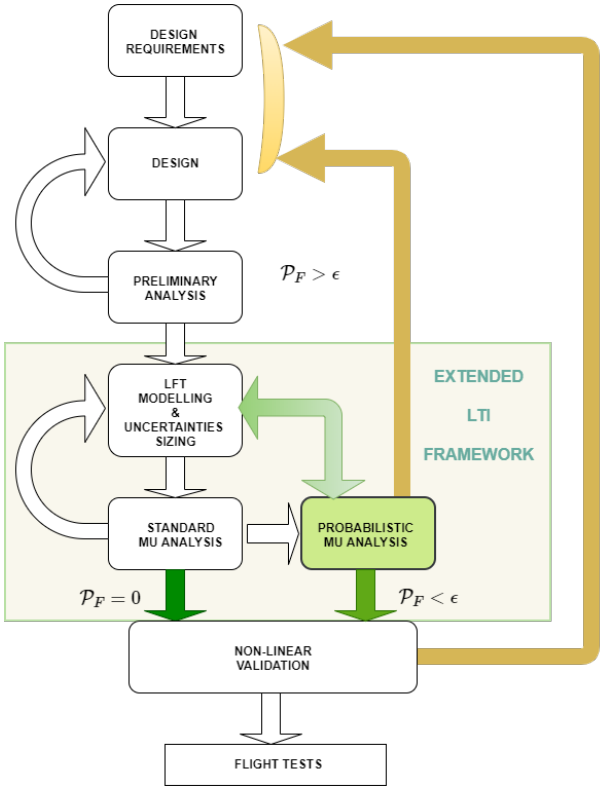

Fig. 11. Integration in a design & validation process

REFERENCES

[1] P. Apkarian, P. Gahinet, and C. Buhr, "Multi-model, multi-objective tuning of fixed-structure controllers," in *ECC*, 2014, pp. 856–861.

[2] G. Balas, P. Seiler, and A. Packard, "Analysis of an UAV flight control system using probabilistic μ," in *Proceedings of the AIAA GNC Conference*, 2012.

[3] J.-M. Biannic and C. Roos, "Generalized State Space: a new Matlab class to model uncertain and nonlinear systems as LFR," available with the SMAC Toolbox at w3.onera.fr/smac/gss, 2012-2020.

[4] F. Boquet, "Active solutions to the spacecraft jitter problem," in *ESA Workshop on Jitter*, 2019.

[5] R. Braatz and M. Morari, "μ-sensitivities as an aid for robust identification," in *Proceedings of the ACC*, 1991, pp. 231–236.

[6] A. Falcoz, D. Alazard, and C. Pittet, "Probabilistic μ-analysis for system performances assessment." *IFAC-PapersOnLine*, vol. 50, no. 1, pp. 399 – 404, 2017, 20th IFAC World Congress.

[7] G. Ferreres, *A practical approach to robustness analysis with aeronautical applications*. Kluwer Academic, 1999.

[8] J. Helton, J. Johnson, C. Sallaberry, and C. Storlie, "Survey of sampling-based methods for uncertainty and sensitivity analysis," *Reliability Engineering and System Safety*, vol. 91, pp. 1175–1209, 2006.

[9] S. Khatri and P. Parrilo, "Guaranteed bounds for probabilistic μ," in *Proceedings of the IEEE CDC*, 1998, pp. 3349 – 3354.

[10] D. Landau and K. Binder, *A guide to Monte Carlo simulations in statistical physics*. Cambridge University Press, 2005.

[11] J. Lesprier, C. Roos, and J.-M. Biannic, "Improved μ upper bound computation using the μ-sensitivities," *IFAC-PapersOnLine*, vol. 48, no. 14, pp. 215 – 220, 2015, 8th IFAC ROCOND Symposium.

[12] A. Marcos, S. Bennani, and C. Roux, "Stochastic μ-analysis for launcher thrust vector control systems," in *Proceedings of the EuroGNC Conference*, 2015.

[13] M. Newlin and P. Young, "Mixed μ problems and branch and bound techniques," *International Journal of Robust and Nonlinear Control*, vol. 7, no. 2, pp. 145–164, 1997.

[14] T. Ott, A. Benoit, P. Van den Braembussche, and W. Fichter, "ESA pointing error engineering handbook," in *ESA GNC Conference*, 2011.

[15] A. Packard and J. Doyle, "The complex structured singular value," *Automatica*, vol. 29, no. 1, pp. 71–109, 1993.

[16] M. Pittelkau, "Definition, metrics and algorithms for displacement, jitter and stability," NASA, Tech. Rep. CP-2003-212246, 2004.

[17] M. Pittelkau and W. McKinley, "Optical transfer functions, weighting functions, and metrics for images with two-dimensional line-of-sight motion," *Optical Engineering*, vol. 55, no. 6, pp. 1 – 17, 2016.

[18] V. Preda, J. Cieslak, D. Henry, S. Bennani, and A. Falcoz, "Robust microvibration mitigation and pointing performance analysis for high stability spacecraft," *International Journal of Robust and Nonlinear Control*, vol. 28, no. 18, pp. 5688–5716, 2018.

[19] C. Roos, "Systems Modeling, Analysis and Control (SMAC) toolbox: An insight into the robustness analysis library," in *Proceedings of the IEEE CACSD Conference*, 2013, pp. 176–181, available with the SMAC Toolbox at w3.onera.fr/smac/smart.

[20] C. Roos and J.-M. Biannic, "A detailed comparative analysis of all practical algorithms to compute lower bounds on the structured singular value," *Control Engineering Practice*, vol. 44, pp. 219–230, 2015.

[21] F. Sanfedino, D. Alazard, V. Pommier-Budinger, F. Boquet, and A. Falcoz, "Dynamic modeling and analysis of micro-vibration jitter of a spacecraft with solar arrays drive mechanism for control purposes," in *Proceedings of the ESA GNC Conference*, 2017.

[22] S. Thai, C. Roos, and J.-M. Biannic, "Probabilistic μ-analysis for stability and H_∞ performance verification," in *Proceedings of the ACC*, 2019, p. 3099–3104.

[23] X. Zhu, "Improved bounds computation for probabilistic μ," in *Proceedings of ACC*, 2000, pp. 4336–4340.

[24] X. Zhu, Y. Huang, and J. Doyle, "Soft vs. hard bounds in probabilistic robustness analysis," in *Proceedings of the IEEE CDC*, 1996, pp. 3412–3417.